forests

MDPI

Article

Modeling Tree Growth Responses to Climate Change: A Case Study in Natural Deciduous Mountain Forests

Mahmoud Bayat [1,*], Thomas Knoke [2], Sahar Heidari [3], Seyedeh Kosar Hamidi [4], Harold Burkhart [5] and Abolfazl Jaafari [1]

[1] Research Institute of Forests and Rangelands, Agricultural Research, Education and Extension Organization (AREEO), Tehran 1496813111, Iran
[2] Institute of Forest Management, TUM School of Life Sciences Weihenstephan, Technical University of Munich, Hans-Carl-von-Carlowitz-Platz 2, 85354 Freising, Germany
[3] Department of Environment, Faculty of Natural Resources, University of Tehran, Tehran 3158777871, Iran
[4] Department of Forestry, Faculty of Natural Resources, Sari Agriculture Sciences and Natural Resource University, Sari 4818166996, Iran
[5] Department of Forest Resources and Environmental Conservation, Virginia Polytechnic Institute and State University, 319 Cheatham Hall, 310 West Campus Drive, Blacksburg, VA 24061, USA
* Correspondence: mbayat@rifr-ac.ir

Abstract: Climate change has significant effects on forest ecosystems around the world. Since tree diameter increment determines forest volume increment and ultimately forest production, an accurate estimate of this variable under future climate change is of great importance for sustainable forest management. In this study, we modeled tree diameter increment under the effects of current and expected future climate change, using multilayer perceptron (MLP) artificial neural networks and linear mixed-effect model in two sites of the Hyrcanian Forest, northern Iran. Using 573 monitoring fixed-area (0.1 ha) plots, we measured and calculated biotic and abiotic factors (i.e., diameter at breast height (DBH), basal area in the largest trees (BAL), basal area (BA), elevation, aspect, slope, precipitation, and temperature). We investigated the effect of climate change in the year 2070 under two reference scenarios; RCP 4.5 (an intermediate scenario) and RCP 8.5 (an extreme scenario) due to the uncertainty caused by the general circulation models. According to the scenarios of climate change, the amount of annual precipitation and temperature during the study period will increase by 12.18 mm and 1.77 °C, respectively. Further, the results showed that the impact of predicted climate change was not very noticeable and the growth at the end of the period decreased by only about 7% annually. The effect of precipitation and temperature on the growth rate, in fact, neutralize each other, and therefore, the growth rate does not change significantly at the end of the period compared to the beginning. Based on the models' predictions, the MLP model performed better compared to the linear mixed-effect model in predicting tree diameter increment.

Keywords: biotic and abiotic factors; climate change; Hyrcanian Forest; machine learning; RCP scenarios

Citation: Bayat, M.; Knoke, T.; Heidari, S.; Hamidi, S.K.; Burkhart, H.; Jaafari, A. Modeling Tree Growth Responses to Climate Change: A Case Study in Natural Deciduous Mountain Forests. *Forests* **2022**, *13*, 1816. https://doi.org/10.3390/f13111816

Academic Editors: Jianfeng Zhang, Honggang Sun and Rongjia Wang

Received: 9 September 2022
Accepted: 26 October 2022
Published: 31 October 2022

1. Introduction

Climate change refers to long-term changes in weather and temperature patterns that may lead to intense drought, flooding, melting polar ice, rising sea levels, water scarcity, severe fire, catastrophic storms, and declining biodiversity [1–4]. Various studies have demonstrated that climate is constantly changing around the world [5] and this change can affect the presence, distribution, and mortality of tree species in forest ecosystems around the world [6]. Such changes can also affect the growth and competition of species. Knowledge of how tree growth can alter with climate change [7] is crucial in providing management options and strategies to adapt to these changes to achieve sustainable forest development [8,9]. Forest growth can be affected directly and indirectly by changes in

precipitation and the occurrence of drought periods. Changes in respiration rate and photosynthesis in response to temperature changes, and through water relations, affect photosynthesis by changing the stomatal conductance [10,11]. To accurately investigate and evaluate these effects, it is necessary to study the influence of simultaneous changes of climate parameters, such as temperature and precipitation on forest attributes, including growth and biodiversity [12,13].

Climate affects several main drivers of forest growth, and the rapid rate of climate change often makes growth prediction uncertain. For example, Strömgren and Linder [14] believe that warmer temperatures increase access to nitrogen and lead to longer growing seasons, which ultimately leads to increased overall production of tree growth and biomass.

Given the rapid increase in temperature and the possibility of increasing the average temperature and precipitation in the world, and since these factors and site conditions have an important effect on forest growth, the assessment of climatic factors in predicting forest growth is very important [12,15]. According to world reports, the annual temperature has increased by 0.07 °C per decade since 1880, and has increased to 0.18 °C since 1981 [16]. There are many concerns about the potential effects of these climate changes on forest functions, such as timber supply, biodiversity, and species distribution, as well as changes in physiological and ecological trends, and tree growth and interactions between species [17–19]. Hamidi et al. [3] investigated the climate change effects on the biodiversity of the Hyrcanian Forest over a long-term period by regression and artificial intelligence models. They concluded that climate change in mountainous areas in the Hyrcanian Forest causes a very slight increase in biodiversity, and did not have a negative effect on biodiversity. The results of this study also showed that the climate change in the Hyrcanian Forest is accompanied by a simultaneous increase in temperature and rainfall. In another study in the Hyrcanian Forest, Limaki et al. [12] investigated the climate change effects on the movement and migration of tree species and concluded that climate change and an increase in air temperature causes the migration of shade-tolerant species, such as beech, to higher elevations in the Hyrcanian Forest.

Individual tree diameter growth models are very important tools in various forest increment and performance systems, because these models are very useful for estimating and predicting the sustainable source of yield, as well as in formulating forest management plans. To determine the current and future rate of forest growth, information about the relative growth and diameter of single trees is required [20,21]. However, little attention has been paid to the climate factors, which is the main factor influencing site productivity. One of the key elements of sustainable forest management is predicting future forest growth and yield under different management scenarios [22]. The projection of future temperature and precipitation is derived from representative concentration pathway (RCP) scenarios, developed for use at the input of the general atmosphere circulation model, and which show the trend of different concentrations of greenhouse gases including carbon dioxide, water vapor, nitrogen oxides, methane, and ozone, which are described in the fifth evaluation report accepted in 2014 [23,24].

Although Bayat et al. [25] and Hamidi et al. [26] studied the growth rate of uneven-aged tree stands in the Hyrcanian Forest, investigations into the effect of climate factors on growth rate still lag behind for this region. To fill this gap in the research, we investigated the effects of biotic and abiotic factors on the tree diameter increment under the effects of current and expected future climate change, using the multilayer perceptron (MLP) artificial neural network and linear mixed-effect model, in two sites of the Hyrcanian Forest. In particular, we address the following questions:

How much do the precipitation and temperature change during the study period?

If climate change occurs, does it have a significant effect on tree diameter increment (negative/positive) or not?

What are the most influential biotic and abiotic factors on the current and future tree diameter increment (under climate change scenarios)?

2. Materials and Methods

2.1. Study Area

The Hyrcanian Forest stretches from the west of the Caspian Sea to the east in a narrow and long strip and spreads in three provinces of Golestan, Mazandaran, and Gilan. The main species in this forest is beech (*Fagus orientalis* Lipsky.), which includes 30% of the tree volume and 30% of the number, and the next species is hornbeam (*Carpinus betulus* L.,), which has the largest number of trees in the forest. Other species include oak (*Quercus castaneifolia*), maple (*Acer velutinum*), and yew species (*Taxus baccata)*; additionally, cypresses (*Juniperus excelsa)* are among the coniferous species of the forest. In this forest, biodiversity indicators increase from west to east [27]. In this study, we studied two sites, i.e., Kheyroud and Farim, from this forest (Figure 1).

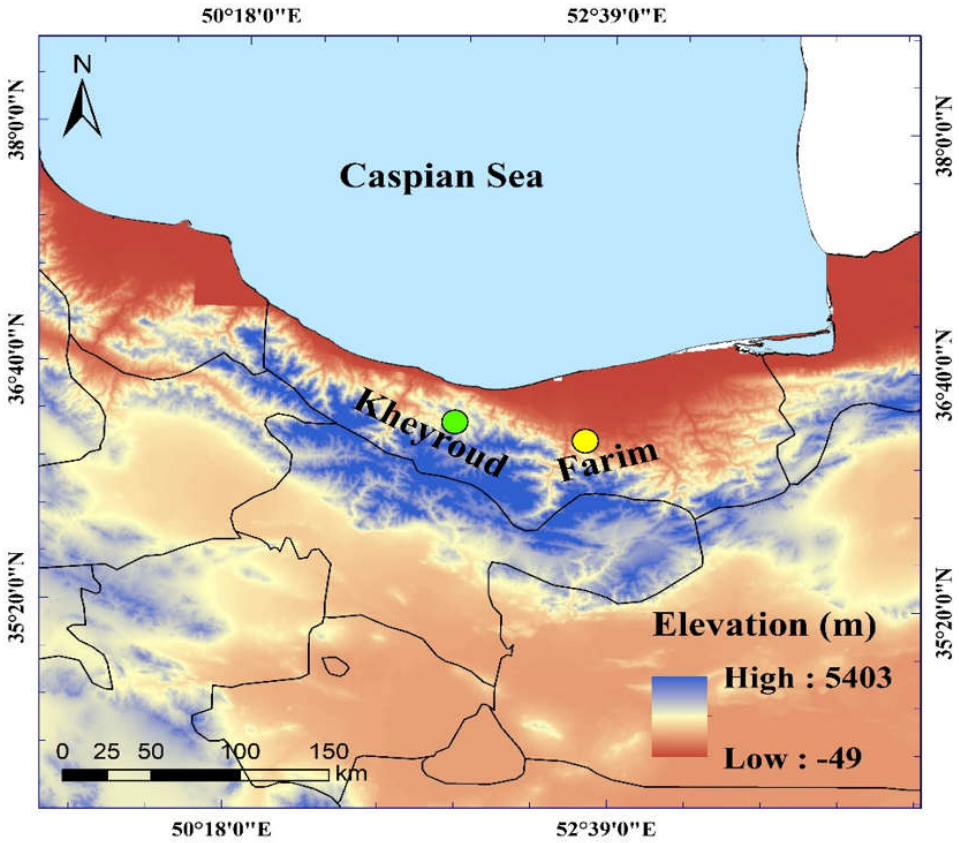

Figure 1. The location of study sites (green and yellow circles) in the Hyrcanian Forest, northern Iran.

In the Kheyroud site, we studied the Gorazbon section, which covers an area of about 934 ha. The elevation of this region is between 980 and 1380 m above sea level and has an average annual temperature of 15.9 °C in the coldest month (February) and 29.2 °C in the warmest month of the year (August). About 1300 mm of precipitation falls annually [24,25].

The Farim site covers an area about 3350 ha with an elevation between 1280 to 1700 m above sea level, and has an average annual precipitation of 845 mm and an annual temperature of 11 °C. Tree species include beech, hornbeam, alder, and elm, and the most important herbaceous species include asparagus, grasses, metametes, violets, cyclamen, and primroses.

2.2. Methodology

The main steps of the methodology proposed in this study are shown in Figure 2 and are summarized as follows.

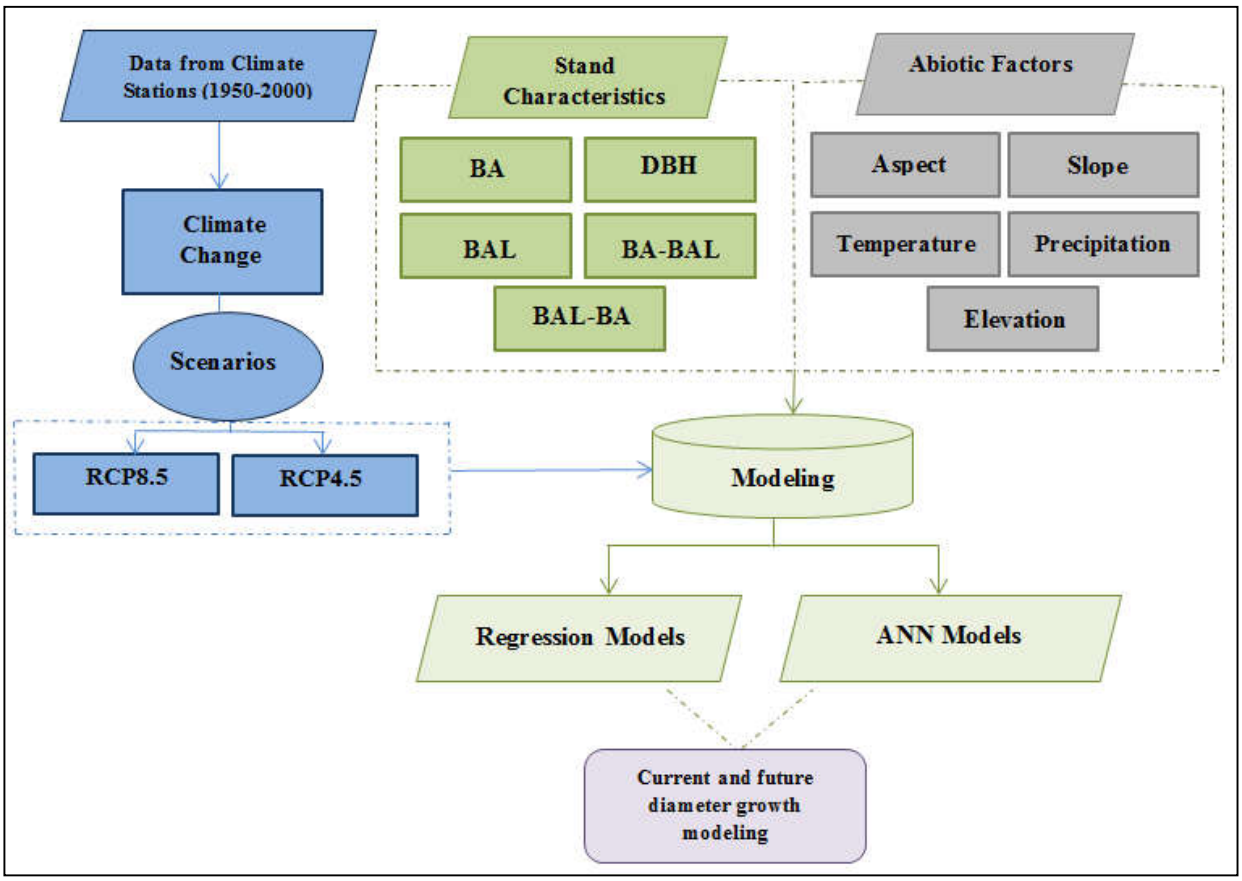

Figure 2. Flowchart of the main research steps. RCP8.5 and RCP4.5 are two scenarios of Representative Concentration Pathway, BA is basal area (m^2 ha^{-1}), BAL is basal area in largest trees (m^2 ha^{-1}), DBH is diameter at breast height (cm), and ANNs is Artificial Neural Networks.

2.3. Data Used

2.3.1. Dependent Variable: Increment Data

In 573 permanent sample plots (0.1 ha), the diameter of all trees with dbh > 7 cm was measured in the same direction in the year 2003 and was re-measured in the year 2012. From the difference between these two measurements, a 10-year diameter increment of trees was obtained [28].

2.3.2. Independent Variables: Climate Data

For each forest site (Kheiroud and Farim), we selected four weather stations that were the closest to these forest sites, and by interpolation we calculated the average temperature and rainfall for each forest site. In this study, more weight was given to the weather stations that were closer to the forest site. Additionally, in this interpolation, we tried to include at least the weather station at a height above sea level equal to the height above sea level of the forest site.

General circulation models are powerful tools to increase the understanding of factors affecting climate and improve the ability to predict future climate patterns. In this study, climatic variables for the period 1950–2000 and the year 2070 (average for 2060–2080) were obtained with a spatial resolution of 1 km^2 from the WorldClim database of the CMIP5 project [29,30]. Precipitation and temperature data was obtained from the interpolation of data from seven meteorological stations nearest to the study sites. In this study, climate scenarios were used to investigate the effect of climate change in 2070 (average for the years 2060 to 2080) and due to the uncertainty caused by the public circulation model under two scenarios, RCP4.5 (an intermediate one) and the RCP8.5 (an extreme one) were used. RCPs climate change scenarios have been developed for use at the input of the

general atmosphere circulation model and show the trend of different concentrations of greenhouse gases (GHG) including carbon dioxide, water vapor, nitrogen oxides, methane, and ozone, which are in the fifth evaluation report accepted in 2014 [12]. These scenarios replaced the GHG Emissions Report (SRES) released in 2000 by the Intergovernmental Panel on Climate Change. According to the RCP 4.5 scenario, global warming is projected to increase by an average of 1.4 °C between 2060 and 2080. According to the IPCC, RCP 4.5 requires that carbon dioxide (CO_2) emissions start declining by approximately 2045 to reach roughly half of the levels of 2050 by 2100 and RCP8.5, generally taken as the basis for worst-case climate change scenarios [3]. First, temperature and precipitation for current and future climatic conditions were extracted under the above two scenarios based on the Hyrcanian Forest boundary within the R software using the raster package. Then, the tree increment rate of the Hyrcanian Forest was calculated based on climatic scenarios in 2070 using the MLP and linear mixed-effect models.

2.3.3. Other Independent Variables

The independent factors used for the diameter increment modeling included tree diameter (DBH), basal area (BA), basal area of large trees (BAL), aspect, slope, elevation, temperature, and precipitation. All independent factors were calculated at the plot level, but the modeling of diameter increment growth was done at the individual tree level.

A brief description of these factors is as follows:

The DBH is the tree diameter at breast height in cm. DBH is one of the most important factors in determining the increment and yield of the forest [31]. Figure 3a shows the distribution of trees to diameter classes in the study sites, with a minimum of 7 and a maximum of 190 cm. Diameter class 15 holds the highest frequency among diameter classes. In this study, the diameter classes are 5 cm and they are continuous. For example, diameter class 15 means all trees from diameter 12.5 to 17.5 are included in this diameter class or diameter class 20 means all trees from diameter 17.5 to 22.5 are included in this diameter class.

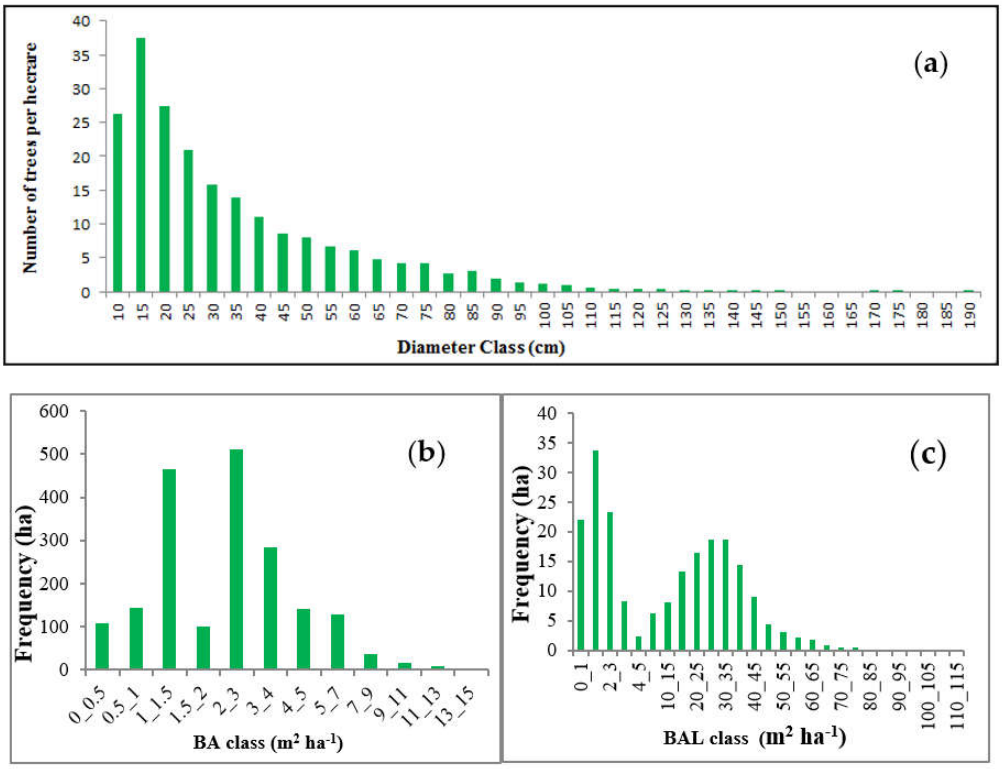

Figure 3. Class frequency of the biotic factors (DBH (**a**), BA (**b**), and BAL (**c**)). DBH is diameter at breast height (cm), BA is basal area (m^2 ha^{-1}), and BAL is basal area in largest trees (m^2 ha^{-1}).

BA is the basal area of a tree that has been measured that corresponds to the tree's DBH. Since this measure is related directly to the volume of the tree, the conversion of DBH to BA is useful and suitable for comparing the dominance of species among different types of forests. BA is expressed as:

$$BA = \frac{\pi}{4} DBH^2 \quad (1)$$

where $\pi = 3.14$.

Figure 3b shows the BA distribution per ha for each plot to the BA classes in the study sites, with a minimum of 0–0.5 and a maximum of 13–15 m^2. Class 2–3 has the highest frequency among classes.

BAL is somehow related to the light available to a tree, because with the increase of BAL, less light is available for neighbor trees. This index provides an effective measure of tree dominance in a stand [32]. BAL is given by:

$$BAL = \frac{\pi}{4} \cdot \sum_{j=1}^{n} \left(tf_j . DBH_j^2 \right) \quad (2)$$

where DBHj > DBHi (i.e., all trees larger than subject tree i), DBH is measured in cm, and tfj is a tree factor (i.e., the number of trees represented by jth tree in a hectare) [32].

Figure 3c shows the BAL distribution per ha for each plot in the study sites, with a minimum of 0–1 and a maximum of 110–115 m^2. Class 2–3 has the highest frequency among classes.

Aspect can affect the access to sunlight, it changes the water and energy balance conditions and causes differences in the structure and composition of vegetation in an area. Figure 4a shows the distribution of aspect classes for each plot over the study area.

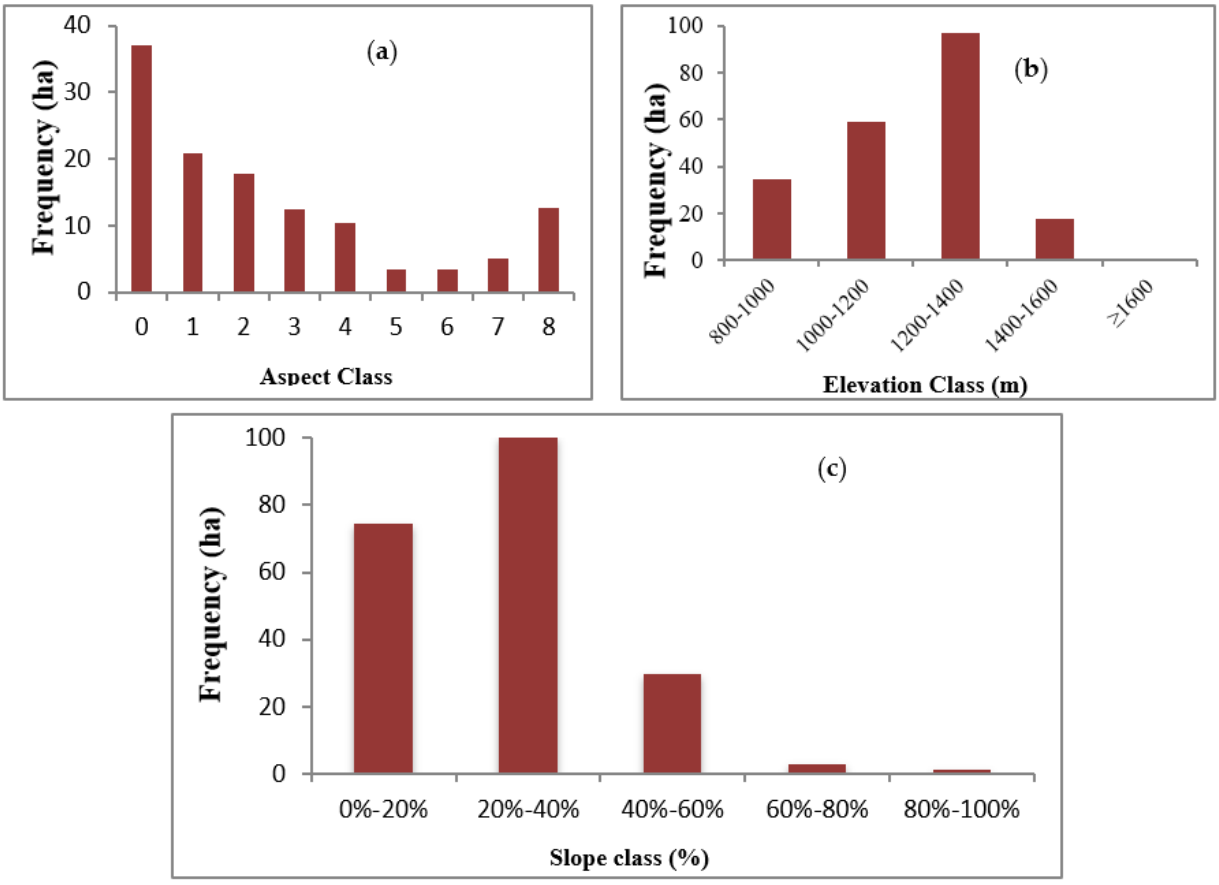

Figure 4. Class frequency of the abiotic factors, aspect (**a**), elevation (**b**), and slope (**c**), over the study area.

Elevation is one of the most important abiotic factors that has an important effect on the structure and distribution of vegetation in an area by affecting other non-living factors. Figure 4b shows the distribution of elevation classes over the study area.

Slope has an important effect on the microclimate because it causes differences in the length of the radiation period in different regions. Together, these factors affect moisture, soil, and other factors, and thus affect the structure and composition of vegetation in an area. Figure 4c shows the distribution of slope classes over the study area.

According to the two climate scenarios used in this study, i.e., RCP 4.5 (an intermediate one) and the RCP 8.5 (an extreme one), the temperature will increase during the periods 2020–2070 about two degrees and precipitation 500 mm, approximately (Figures 5 and 6).

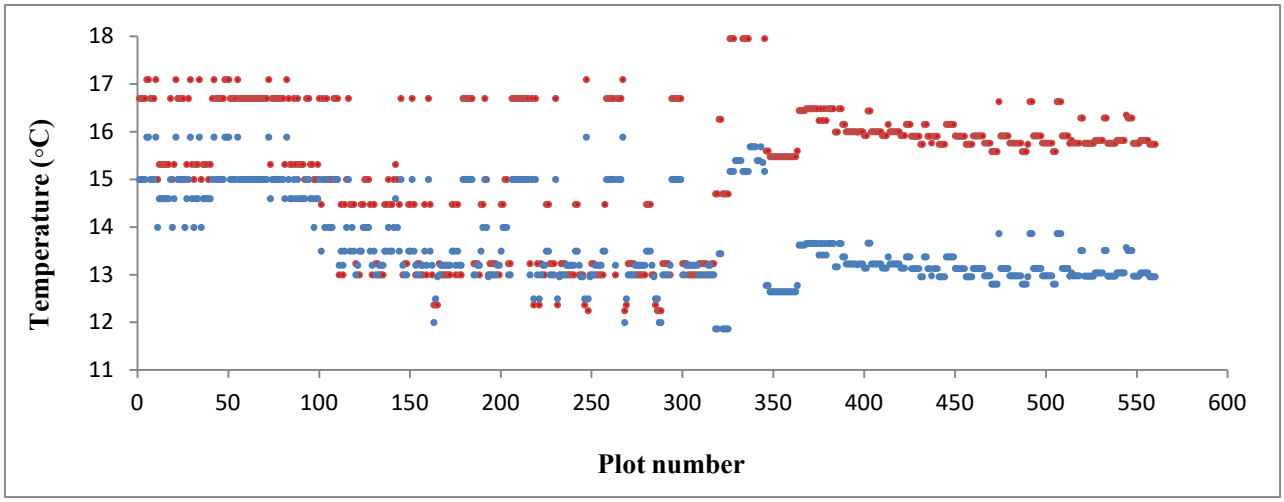

Figure 5. The trend of annual temperature changes at the beginning (blue points) and end (red points) of the period in the studied plots.

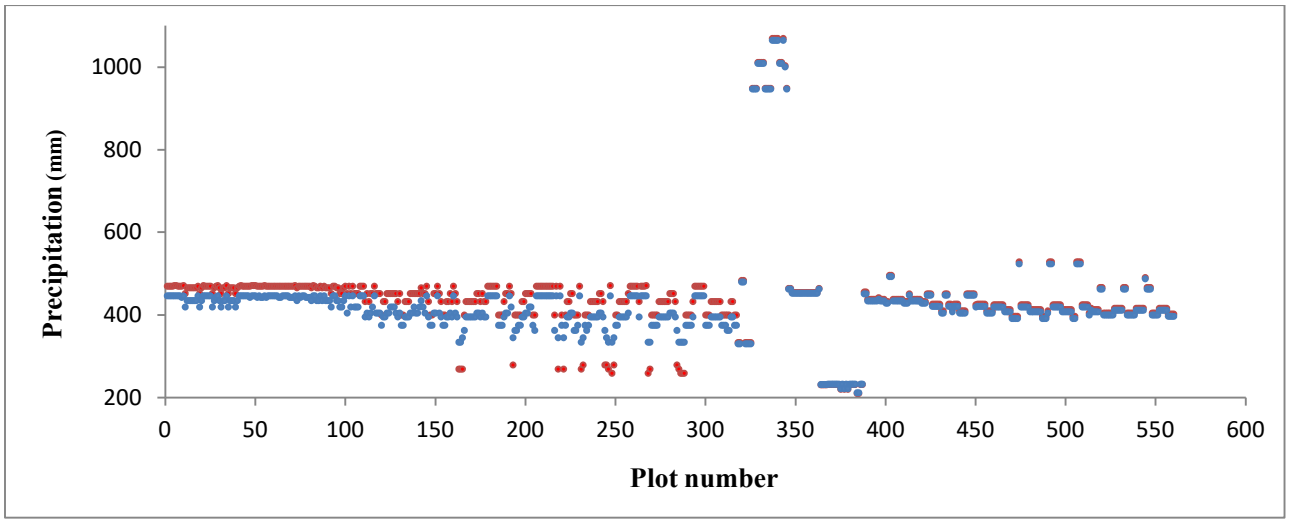

Figure 6. The trend of annual precipitation changes at the beginning (blue points) and end (red points) of the period in the studied plots.

2.4. Models Used

The models used in this study were the MLP and linear mixed-effect models. A brief description of these models is as follows.

The linear mixed-effect model can simultaneously model fixed and random effects. In these models, predictors are used to represent group membership. The coefficients for each group in the data are then estimated. A linear mixed-effect model can be expressed as:

$$y = X\beta + Zu + \varepsilon \quad (3)$$

where y is a N × 1 column vector, the dependent variable, X is a N × p matrix of the p predictor (independent) variables, β is a p × 1 column vector of the fixed-effects regression coefficients (the βs), Z is a N × qJ design matrix for the q random effects and J groups, u is a qJ × 1 vector of q random effects (the random complement to the fixed β) for groups, and ε is a N × 1 column vector of the residuals that part of y that is not explained by the model, in this study, physiographic, climatic and biometric variables were considered as fixed effect and plots as random effect.

MLP is a method for modeling that can be used in relation to conventional modeling due to their intelligent structure and flexibility in accepting conventional modeling [26]. In this study, we used a multilayer perceptron (MLP) class for modeling tree growth.

Model Training and Validation

The training stage was performed to determine the optimal network structure, weight matrix, and threshold matrix. For this purpose, we randomly divided the data into two groups and used 70% for model training. We used the remaining 30% of the data and employed three validation criteria including RMSE, RMSE%, and BIAS, to evaluate the predictive accuracy of the models. The validation criteria are calculated as follows [33]:

$$\text{BIAS} = \frac{\sum_{i=1}^{n}(\hat{y}_i - y_i)}{n} \quad (4)$$

$$\text{RMSE} = \sqrt{\sum_{i=1}^{n} \frac{(y_i - \hat{y}_i)^2}{n-k}} \quad (5)$$

$$\%\text{RMSE} = 100 \times \sqrt{\sum_{i=1}^{n} \frac{(y_i - \hat{y}_i)^2}{n-k}} / \overline{y} \quad (6)$$

where n is the number of observations, y_i is the observed value, $\hat{y}_i$ is the estimated value, $\overline{y}$ is the mean of the observed value, and k is the number of parameters [34].

3. Results

3.1. Modeling Results for Each Species

3.1.1. Fagus

$$\begin{gathered} DI = 13.86 + uj + 0.03\ (DBH) - 1.24\ (BA) + 0.0072\ (BAL) \\ 0.0016\ (ASP) - 0.0027\ (ELE) - 0.77\ (TEMP) + 0.0022\ (PRPE) + eij \end{gathered} \quad (7)$$

The standard deviation and variance for the random factor of species were 0.26 and 0.11, respectively. The RMSE, bias, and R^2 were 1.66 cm, 1.39 cm, and 0.20, respectively, with a 95% confidence (Table 1).

3.1.2. Carpinus

$$\begin{gathered} DI = 6.51 + uj + 0.04\ (DBH) - 2.23\ (BA) - \\ 1.04\ (BA\text{-}BAL) + 1.04\ (BAL\text{-}BA) + 0.0011(ASP) - \\ 0.0013\ (ELE) - 0.30\ (TEMP) + 0.00052\ (PRPE) + eij \end{gathered} \quad (8)$$

The standard deviation and variance for the random factor of species were 0.43 and 0.21, respectively. The RMSE, bias, and R^2 were 1.74 cm, 1.64 cm, and 0.10, respectively, with a 95% confidence (Table 2).

Table 1. Results of the linear mixed-effect model for Fagus diameter increment.

Fagus	Estimate	Std. Error	t Value	Pr (>|t|)
Intercept	13.86678	1.202374	11.5328	0.000000
DBH	0.03621	0.003532	10.2515	0.000000
BA	−1.24626	0.372723	−3.3437	0.000833
BAL	0.00724	0.001901	3.8095	0.000141
BA_BAL	−0.11809	0.124150	−0.9512	0.341546
BAL_BA	−0.00004	0.000022	−1.7320	0.083342
ASP	0.00169	0.000306	5.5352	0.000000
SLP	0.00031	0.001607	0.1940	0.846222
ELE	−0.00272	0.000265	−10.2758	0.000000
TEMP	−0.77897	0.072303	−10.7738	0.000000
PREC	0.00226	0.000321	7.0347	0.000000

DBH is diameter at breast height, BA is basal area, BAL is basal area in largest trees, ASP is aspect, SLP is slope, ELE is elevation, TEMP is temperature, and PREC is participation.

Table 2. Results of the linear mixed-effect model for Carpinus diameter increment.

Carpinus	Estimate	Std. Error	t Value	Pr (>|t|)
Intercept	6.51818	0.801555	8.13192	0.000000
DBH	0.04583	0.004726	9.69805	0.000000
BA	−2.23963	0.604983	−3.70198	0.000217
BAL	0.00041	0.001998	0.20604	0.836767
BA_BAL	−1.04600	0.287918	−3.63298	0.000284
BAL_BA	0.00008	0.000011	7.16247	0.000000
ASP	0.00110	0.000298	3.68348	0.000233
SLP	−0.00243	0.002056	−1.18355	0.236659
ELE	−0.00137	0.000218	−6.26503	0.000000
TEMP	−0.30486	0.048397	−6.29913	0.000000
PREC	0.00052	0.000221	2.35220	0.018710

DBH is diameter at breast height, BA is basal area, BAL is basal area in largest trees, ASP is aspect, SLP is slope, ELE is elevation, TEMP is temperature, and PREC is participation.

3.1.3. Quercus

$$\begin{gathered} DI = 11.23 + uj + 0.08\ (DBH) - \\ 5.49\ (BA) + 0.02\ (BAL) - \\ 0.0014\ (ELE) - 0.65\ (TEMP) + eij \end{gathered} \quad (9)$$

The standard deviation and variance for the random factor of species were 0.21 and 0.08, respectively. The RMSE, bias, and R^2 were 1.64 cm, 1.37 cm, and 0.24, respectively, with a 95% confidence (Table 3).

Table 3. Results of the linear mixed-effect model for Quercus diameter increment.

Quercus	Estimate	Std. Error	t Value	Pr (>|t|)
Intercept	11.23192	2.848557	3.94302	0.000091
DBH	0.08955	0.018065	4.95705	0.000001
BA	−5.49099	2.172556	−2.52743	0.011780
BAL	0.02703	0.009387	2.87913	0.004149
BA_BAL	−0.47566	0.648376	−0.73362	0.463506
BAL_BA	−0.00011	0.000085	−1.28709	0.198626
ASP	−0.00009	0.000994	−0.09118	0.927383
SLP	−0.00168	0.005095	−0.32890	0.742362
ELE	−0.00140	0.000695	−2.00836	0.045113
TEMP	−0.65842	0.158488	−4.15439	0.000038
PREC	0.00025	0.000856	0.28801	0.773449

DBH is diameter at breast height, BA is basal area, BAL is basal area in largest trees, ASP is aspect, SLP is slope, ELE is elevation, TEMP is temperature, and PREC is participation.

3.1.4. Others Species

$$DI = 12.37 + uj + 0.02\ (BAL) - 0.0003\ (BAL\text{-}BA) - 0.0014\ (ELE) - 0.63\ (TEMP) + eij \quad (10)$$

The standard deviation and variance for the random factor of species were 0.16 and 0.19, respectively. The RMSE, bias, and R^2 were 1.70 cm, 1.60 cm, and 0.12, respectively, with a 95% confidence (Table 4). Tables 5 and 6 show the most important characteristics of MLP-based ANNs and associated metrics for diameter model training and evaluation by species.

Table 4. Results of the linear mixed-effect model for others species diameter increment.

Others Species	Estimate	Std. Error	t Value	Pr (>|t|)
Intercept	12.37578	1.823423	6.78711	0.000000
DBH	0.00689	0.006085	1.13154	0.257977
BA	0.96779	0.602838	1.60539	0.108578
BAL	0.02499	0.004180	5.97897	0.000000
BA_BAL	−0.44267	0.386819	−1.14440	0.252608
BAL_BA	−0.00033	0.000055	−5.99956	0.000000
ASP	−0.00010	0.000581	−0.16392	0.869808
SLP	0.00043	0.002916	0.14735	0.882876
ELE	−0.00142	0.000462	−3.06661	0.002196
TEMP	−0.63779	0.102897	−6.19840	0.000000
PREC	0.00087	0.000479	1.82720	0.067831

DBH is diameter at breast height, BA is basal area, BAL is basal area in largest trees, ASP is aspect, SLP is slope, ELE is elevation, TEMP is temperature, and PREC is participation.

Table 5. The most important characteristics of MLP-based ANNs and associated metrics for diameter model training by species.

Species	Network Name	Algorithm	Error Function	Hidden Activation	R^2	RMSE	% RMSE	BIAS	% BIAS
Fagus	MLP 10-6-1	BFGS 46	SOS	Logistic	0.50	0.43	18.69	0.0005	0.029
Carpinus	MLP 10-4-1	BFGS 53	SOS	Tanh	0.37	0.69	31.08	0.0025	0.079
Quercus	MLP 10-12-1	BFGS 26	SOS	Logistic	0.57	0.40	17.77	0.0004	0.026
Others	MLP 10-11-1	BFGS 33	SOS	Exponential	0.42	0.58	26.24 s	0.0017	0.030

Table 6. The most important characteristics of MLP-based ANNs and associated metrics for diameter model evaluation by species.

Species	Network Name	Algorithm	Error Function	Hidden Activation	R^2	RMSE	% RMSE	BIAS	% BIAS
Fagus	MLP 10-6-1	BFGS 46	SOS	Logistic	0.47	0.50	22.52	0.0009	0.006
Carpinus	MLP 10-4-1	BFGS 53	SOS	Tanh	0.41	0.61	27.47	0.0028	0.017
Quercus	MLP 10-12-1	BFGS 26	SOS	Logistic	0.58	0.41	18.56	0.0006	0.004
Others	MLP 10-11-1	BFGS 33	SOS	Exponential	0.42	0.63	28.12	0.0023	0.011

3.2. Modeling Results for the Current Conditions

The application of the linear mixed-effect model provided the following equation for the estimation of the tree diameter increment (DI).

$$\begin{gathered} DI = 1.17 + u_j + 4.39\ (DBH) - 2.20\ (BA) - \\ 0.032\ (BA/BAL) - 0.00029\ (BAL/BA) - \\ 0.0022\ (elevation) + 0.0021\ (aspect) - \\ 0.62\ (temperature) + 0.0014\ (precipitation) + e_{ij} \end{gathered} \quad (11)$$

The standard deviation and variance for the random factor of species were 0.30 and 0.09, respectively. The RMSE, bias, and R^2 were 1.61 cm, 1.33 cm, and 0.25, respectively, with a 95% confidence. According to Table 7, all the variables except the slope and basal area of the thickest trees are significant in the model Figure 7 represents the relationship between the predicted and actual diameter increment using the regression model.

Table 7. Results of the linear mixed-effect model for diameter increment.

	Estimate	Std. Error	t Value	Pr (>|t|)
Intercept	1.176×10^{1}	$1.134e \times 10$	10.367	$<2 \times 10^{-16}$ ***
DBH	4.393×10^{-2}	2.440×10^{-3}	18.001	$<2 \times 10^{-16}$ ***
BA	-2.201×10	2.645×10^{-1}	−8.323	$<2 \times 10^{-16}$ ***
BAL	-1.846×10^{-3}	1.901×10^{-3}	−0.971	0.33195
BA_BAL	-3.250×10^{-1}	1.071×10^{-1}	−3.035	0.00241 **
BAL_BA	2.958×10^{-5}	9.427×10^{-6}	3.138	0.00171 **
ASP	2.157×10^{-3}	3.677×10^{-4}	5.865	8.88×10^{-9} ***
ELE	-2.219×10^{-3}	2.698×10^{-4}	−8.223	2.22×10^{-15} ***
SLP	-3.050×10^{-3}	2.003×10^{-3}	−1.523	0.12846
TEMP	-6.222×10^{-1}	6.650×10^{-2}	−9.356	$<2 \times 10^{-16}$ ***
PREC	1.488×10^{-3}	3.137×10^{-4}	4.744	2.83×10^{-6} ***

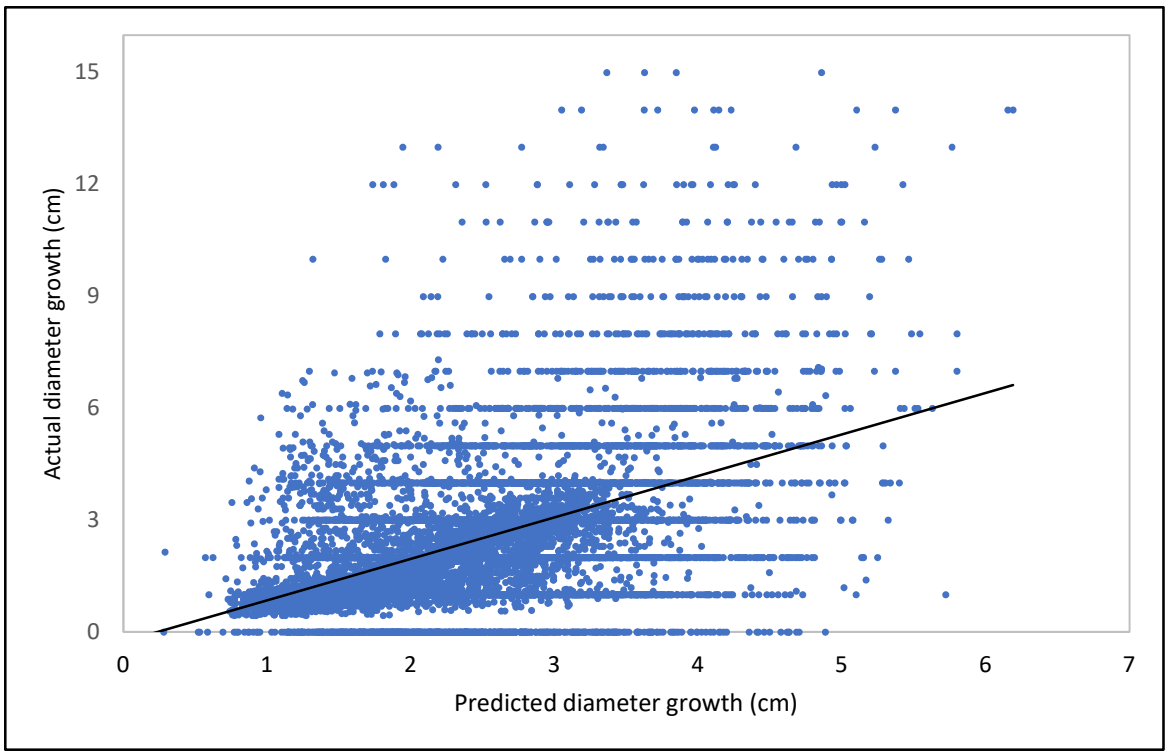

Figure 7. The relationship between predicted and actual diameter increment extracted by the mixed-effect model.

Table 8 shows the results of the application of the MLP model with different net-works in the training and validation steps and only the models with high accuracy are given, while the results of all ANN are given in the Supplemental Materials (Tables S1 and S2). Figure 8 represents the relationship between the predicted and actual diameter increment using the MLP model artificial neural network.

Table 8. The results of the MLP model for the training and validation step.

Sample	Network	Algorithm	Error Function	Hidden Activation	R^2	RMSE	% RMSE	BIAS	% BIAS
Train	MLP 10-9-1	BFGS 106	SOS	Tanh	0.48	0.52	21.84	0.0008	0.0336
Validation	MLP 10-9-1	BFGS 106	SOS	Tanh	0.44	0.63	26.47	0.0010	0.04201

MLP = multilayer perceptron (10-7-1 implies 10 = number of input layers; 7 = number of hidden layers; and 1 = number of output layer); BFGS = Broyden-Fletcher-Goldfarb-Shanno; RBFT = Radial Basis Function Training; SOS = Symbiotic Organisms Search.

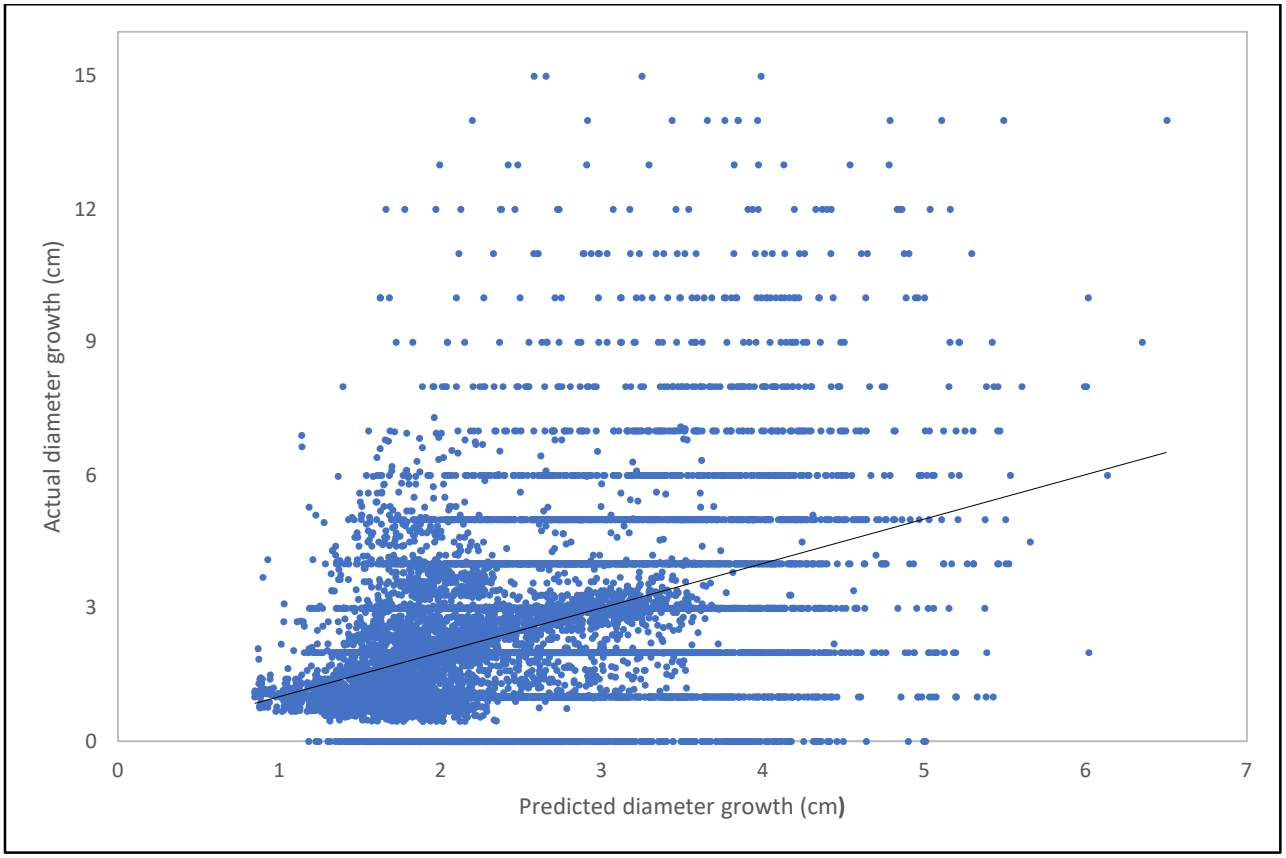

Figure 8. The relationship between predicted and actual diameter increment extracted by the MLP model.

The most influential factors in the MLP model are elevation, BAL, aspect, temperature, and DBH (Figure 9).

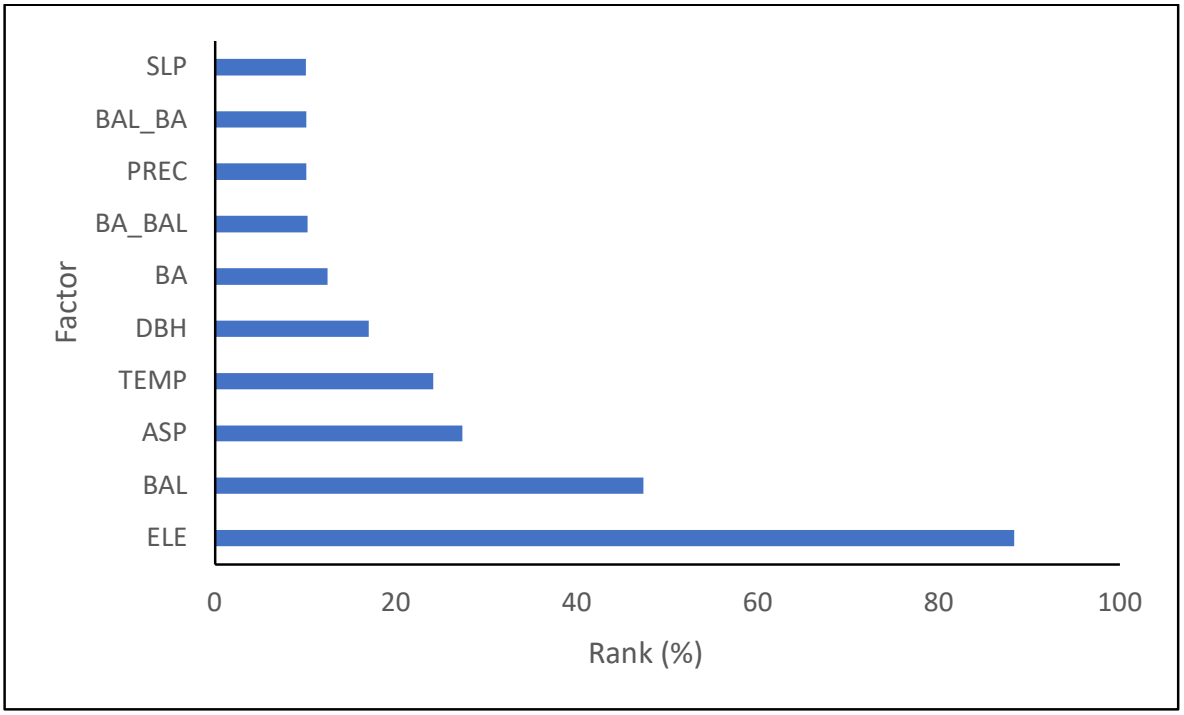

Figure 9. Relative importance of the predictor factors measured by the MLP model. SLP is slope, BA is basal area, BAL is basal area in largest trees, PREC is participation, DBH is diameter at breast height, TEMP is temperature, ASP is aspect, and ELE is elevation.

3.3. Modeling Results for the Next 50 Years

The results of linear mixed-effect model for the diameter increment for the next 50 years (DIf) are as follows:

$$\begin{aligned} \text{DIf} = &- 3.12 + \text{uj} + 4.45\ (\text{DBH}) - 2.28\ (\text{BA}) - \\ &0.031\ (\text{BA/BAL}) + 0.00306\ (\text{BAL/BA}) + \\ &0.0101\ (\text{elevation}) + 0.0028\ (\text{aspect}) + \\ &0.234\ (\text{precipitation}) - 0.0123\ (\text{PREC}) + \text{eij} \end{aligned} \quad (12)$$

The standard deviation and variance for the random factor of species were 0.28, and 0.08, respectively. The RMSE, bias, and R^2 were 1.54 cm, 1.27 cm, and 0.30, respectively, at significance level 95% (Figure 10, Table 9).

Table 9. Results of regression model analysis for diameter growth of trees under change climate.

Variable	Estimate	Std. Error	t Value	Pr (>|t|)
Intercept	-3.128×10	9.376×10^{-1}	−3.337	0.000911 ***
DBH	4.453×10^{-2}	2.451×10^{-3}	18.169	$<2 \times 10^{-16}$ ***
BA	-2.282×10	2.657×10^{-1}	−8.589	$<2 \times 10^{-16}$ ***
BAL	-1.825×10^{-3}	2.057×10^{-3}	−0.887	0.375212
BA_BAL	-3.312×10^{-1}	1.075×10^{-1}	−3.081	0.002065 **
BAL_BA	3.066×10^{-5}	9.440×10^{-6}	3.248	0.001166 **
ASP	2.877×10^{-3}	3.820×10^{-4}	7.531	2.90×10^{-13} ***
ELE	1.011×10^{-3}	2.944×10^{-4}	3.435	0.000644 ***
SLP	-1.393×10^{-3}	2.146×10^{-3}	−0.649	0.516438
TEMP	2.346×10^{-1}	4.451×10^{-2}	5.272	2.00×10^{-7} ***
PREC	-1.232×10^{-3}	2.880×10^{-4}	−4.277	2.33×10^{-5} ***

DBH is diameter at breast height, BA is basal area, BAL is basal area in largest trees, ASP is aspect, SLP is slope, ELE is elevation, TEMP is temperature, and PREC is participation. ** $p \leq 0.01$*** $p \leq 0.001$.

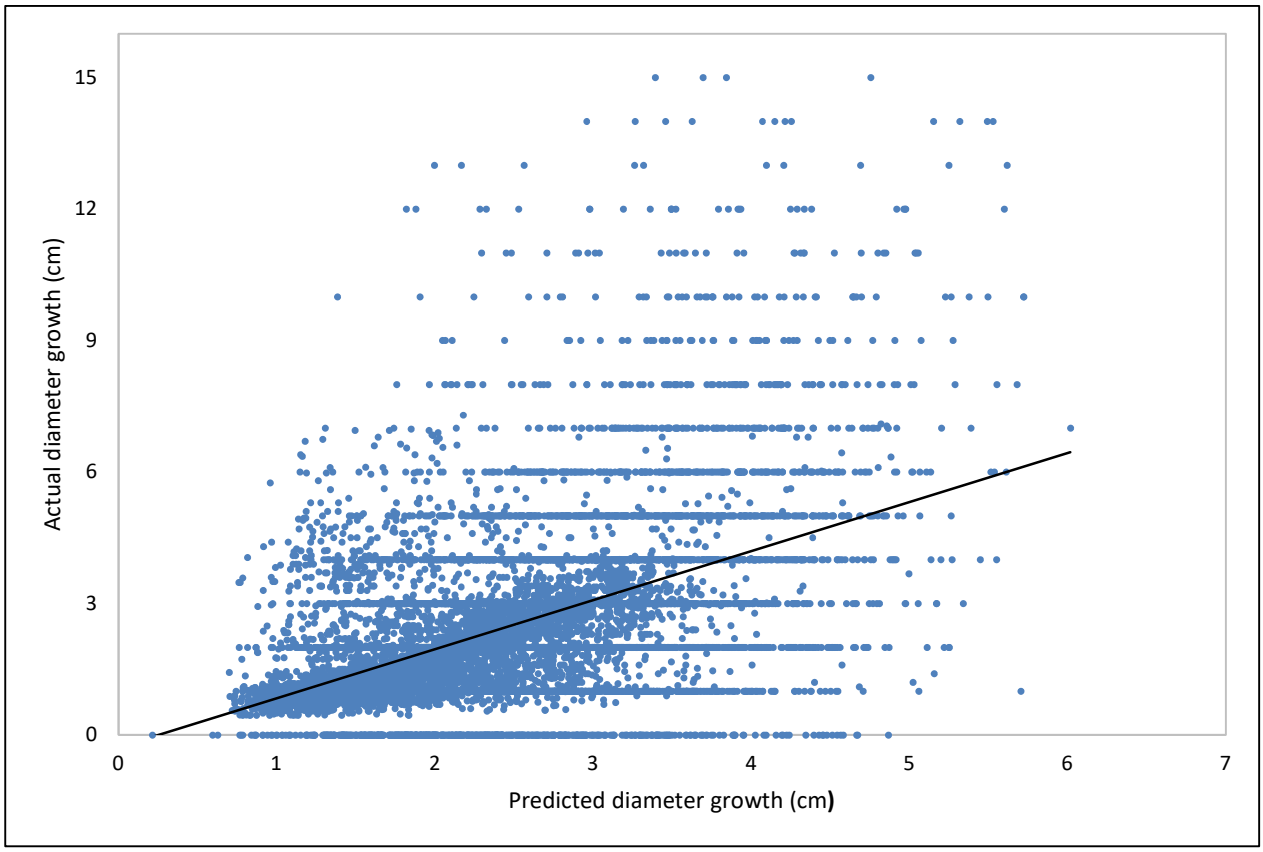

Figure 10. Relationship between predicted and actual diameter increment by mixed-effect regression (cm) affected by climate change.

In Table 10 the results of the neural network model, the MLP algorithm with lower RMSE and BIAS is more suitable than the RBF model and the models with high accuracy are given, while the performance of all deter-mined ANNs is provided in the Supplemental Materials (Tables S3 and S4). In addition, Figure 11 represents the relationship between the predicted and actual diameter increment for all species by ANN.

Table 10. Characteristics of RBF and MLP-based ANNs and associated metrics for diameter model training and validation.

Sample	Network	Algorithm	Error Function	Hidden Activation	R^2	RMSE	% RMSE	BIAS	% BIAS
Train	MLP 10-11-1	BFGS 196	SOS	Exponential	0.49	0.50	20.92	0.0005	0.020
Validation	MLP 10-11-1	BFGS 196	SOS	Exponential	0.44	0.76	31.79	0.0019	0.079

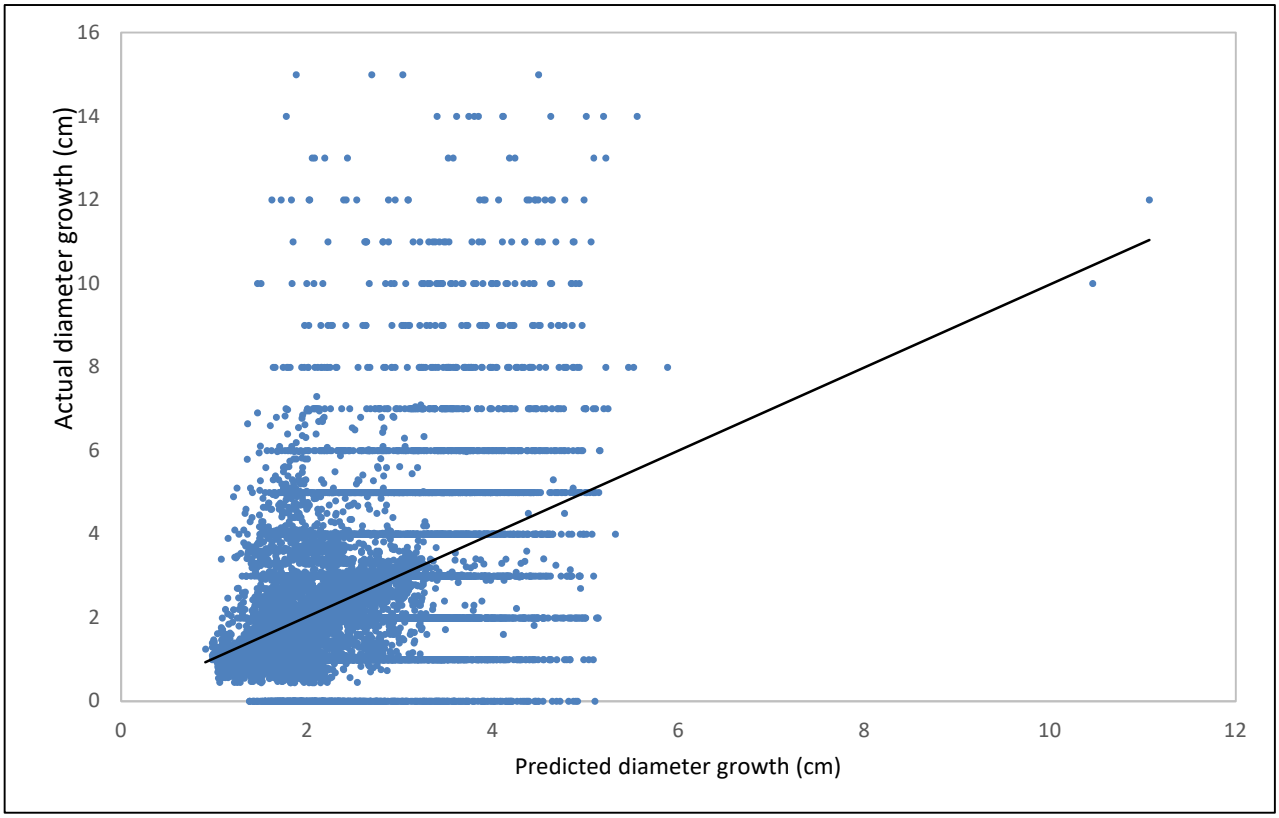

Figure 11. Relationship between predicted and actual diameter increment for future time by ANN (cm) affected by climate change.

The influential factors in this method are DBH, basal area, basal area large, aspect, temperature, elevation, ratio basal area large to basal area, precipitation, ratio basal area to basal area large, and slope (Figure 12).

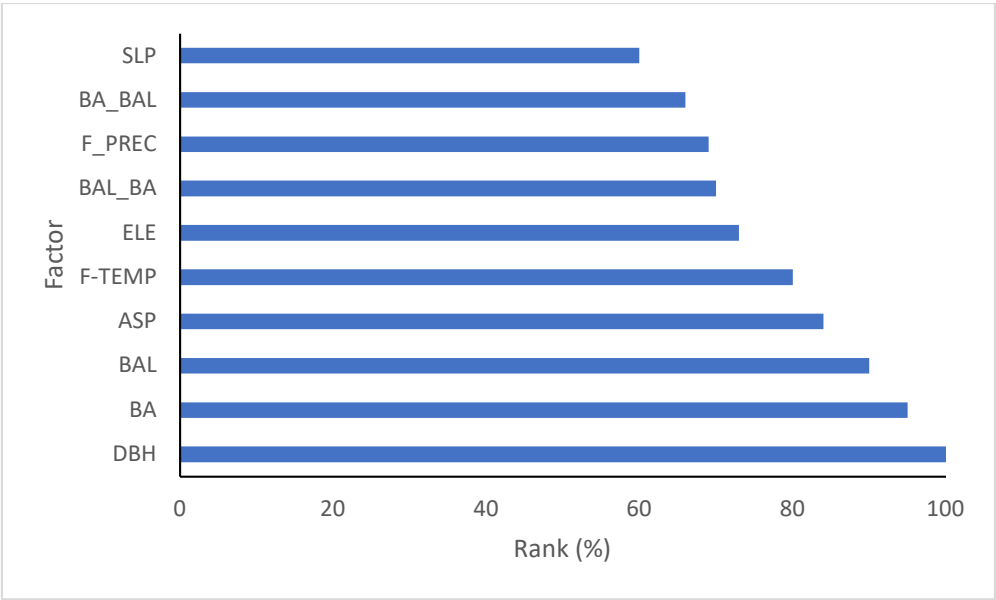

Figure 12. Relative importance of predictor factors in the ANN model for future diameter increment. SLP is slope, BA is basal area, BAL is basal area in largest trees, PREC is participation, DBH is diameter at breast height, TEMP is temperature, ASP is aspect, and ELE is elevation.

Table 11 shows the diameter increment changes from the current to 2070 under climate change. The results show that due to changes in precipitation and temperature in the region, the amount of diameter increment model is decreasing in the forest region.

Table 11. Changes in individual diameter increment (cm) by regression and artificial neuron network under climate change.

Climate Condition	Species	Linear Mixed-Effect Model	MLP
Current	Fagus	2.30	2.31
	Carpinus	2.22	2.24
	Quercus	2.96	2.98
	Other	2.85	2.86
	All	2.39 (cm)	2.40 (cm)
Future time	Fagus	2.30	2.31
	Carpinus	2.22	2.25
	Quercus	2.94	2.98
	Other	2.85	2.86
	All	2.38 (cm)	2.39 (cm)

MLP is multilayer perceptron.

4. Discussion

Estimating forest increment is one of the most important stages of forest management planning [25]. Thus, the accuracy of this estimation is very important. In this study, using individual tree models, we estimated the effect of biotic and abiotic factors on the increment of tree species in Hyrcanian Forest under climate change conditions These models are actually a series of mathematical equations or interconnected equation systems that can provide future forest increment with any combination of inputs for optimal forest management. In this regard, we used different structures of the ANN model and the linear mixed-effect model. Compared to the ANN models, the linear mixed-effect model had a higher RMSE (i.e., modeling error). Many researchers have used ANN models in forestry for the simulation of the forest growth process and found them effective models [27,35]. Despite the efficiency of artificial intelligence, linear mixed-effect models also have advantages that can be used as a complement to other models [21]. For example, ANN makes fewer assumptions about data, [26,36], has higher flexibility and accuracy, the ability to model nonlinear and complex relationships, and the ability to clearly display the relationships between variables [31].

The results of the factor importance analysis showed that elevation and BAL had the greatest relative importance in estimating increment in different structures of ANN. Further, BAL was used to account for competition. This index is one of the best and most usual indicators for calculating one-side competition in forest ecosystems because it is relatively simple to calculate, has a good correlation with growth rate, and it is an absolute value [37,38]. In general, the results of factor analysis showed that the abiotic factors had a much greater effect on increment estimation than biotic factors. In line with our results, Primicia et al. [39] concluded that elevation in the two-way interaction with the competition factor is one of the most important factors in the response of trees to the climate. Of course, this response is also affected by the tree age such that older trees are more sensitive to climate change than young trees, and their response to the effect of climate depends on elevation. It should be noted that our study was in the forest with un-even aged stands, so, did not consider the age factor.

The RCP4.5 and RCP8.5 scenarios projected increased temperature and precipitation for the year 2070. The annual average temperature is 13.75 °C in the year 2020 and will reach 15.52 °C in the year 2070. Additionally, the average of annual precipitation in year 2020 is 425.01 mm and will increase to 437.19 mm in the year 2070. Unlike biodiversity, which has an increasing trend from west to east of the Caspian Sea [27], the rate of diameter increment is decreasing, and this can be a result of reduced precipitation. Accordingly, the rate of tree increment in the forest of the region under the RCP4.5 scenarios is decreased by 0.01

and 7.5%. Temperature on the southern slopes of the Caspian Sea has increased in recent years [40], which reduces snow cover, slows down and reduces surface and subsurface humidity, and creates drought conditions for vegetation in most years. As our findings show, we are witnessing a significant increase in temperature and precipitation in the Hyrcanian Forest. However, due to the increase in temperature and precipitation in 2070, the tree increment rate is projected to decrease slightly.

In this study, the diameter increments for each species, such as the diameter increment of the beech, the diameter increments of the hornbeam, and the diameter increment for the total species, which is the productivity of the forest, was calculated for the current conditions and under the influence of climate change; the results showed that in both cases climate change did not affect the growth and productivity of the forest. In fact, the simultaneous increase of rainfall and air temperature prevents the occurrence of a very severe disturbance in the diameter increment of trees in the Hyrcanian mountain forests. In line with our results, Burkhart et al. [41] confirmed that the climate does not have much effect on growth, but the increase in CO_2 causes growth to increase. In fact, the increased levels of CO_2 have two effects: (1) climate, and (2) tree physiological efficiency (photosynthesis, water uptake, nutrient uptake, etc.).

Given several studies worldwide, the response of different species to the impact of climate change is different. For example, studies in Ontario, Canada, showed that the effects of projected climate change were positive in the northwest and northeast for jack pine and negative and neutral in the center west and far west for red pine, respectively [42]. However, drought stress may affect plant increment, if the increase in temperature is not accompanied by an increase in precipitation [43,44]. Studies on tree species such as grown balsam fir (*Abies balsamea* (L.) Mill.), black spruce (*Picea mariana* (Mill.) B.S.P.), jack pine (*Pinus banksiana* Lamb.), and trembling aspen (*Populus tremuloides* Michx.) in the Eastern Canadian region have shown that the average annual temperature affects the basal area of these tree species [43].

In this regard, several studies have been conducted, each of which has presented different results in relation to increasing or decreasing the increment rate of the tree with precipitation and temperature changes. For example, Goldblum and Rigg [45] reported that when precipitation and temperature increased on the northeastern coast of Lake Superior in Ontario, Canada, the increment rate of sugar maple and white spruce increased. However, diameter increment of balsam was not affected by higher temperatures in the fall. Subedi and Sharma [42] also reported the same results; they used 30-year increment data (1971–2000) and concluded that the climate change had positive and negative effects on the diameter increment of jack pine and black spruce trees, respectively. Oboite and Comeau [46] developed climate-sensitive mixed effects models for some tree species in Canada; they reported a negative effect on coniferous trees during the frost-free period and an increase in increment on deciduous trees with longer frost-free period. Further, more moisture increased the increment of trees, but the effect of available moisture depended on the competitive factor. Sharma [43] modeled diameter increments for red pine plantations in a changing climate and concluded that the projected diameters for trees in the southeast and southwest were 11 and 23% larger, respectively, and for trees in the west-central region 6% narrower at the end of the growing period, 2021–2080. Yang et al. [15] in the Taihang Mountains, Northern China, examined the factors affecting the increment of trees under climate change and concluded that the combination of increasing temperature and precipitation has a decreasing effect on the increment rate, which is exactly the same as the results of the present study, but they also suggested that the accuracy of the prediction could be increased if we evaluated the species separately. Further, precipitation had a positive effect on forest increment. Laubhann, et al. [47] studied the effect of temperature, precipitation, and the deposition change of sulphur and nitrogen compounds on forest increment. They analyzed *Fagus sylvatica*, *Quercus petraea*, and *Q. robur*, *Pinus sylvestris*, and *Picea abies*. Their results are in line with ours; they concluded for all species, except *Picea abies*, the increasing temperature had a positive influence on increment.

Particular tree species may respond differently to climate change across any region. In this study, we studied oriental beech (*Fagus orientalis* Lipsky), common hornbeam (*Carpinus betulus* L.), Caucasian alder (*Alnus subcordata* C.A. Mey), velvet maple (*Acer velutinum* Boiss.), and large-leaved lime tree (*Tilia platyphyllos* Scop.) and assumed responding to climate change in forest increment for all populations are similar.

Given the fact that the increment rate has not changed significantly during the study period, as seen in various previous works (e.g., [15]), increasing the temperature on one hand, with increasing evapotranspiration, reduces the increment rate and increases precipitation also increases the rate in another hand. However, according to the prediction of climate change scenarios studied in this research, during the study period, an increase in temperature and precipitation will occur together, so these two effects neutralize each other on the increment rate and thus the increment rate at the end of the period has not changed significantly.

5. Conclusions

In this study, we investigated the effect of climate change, which was simulated with the RCP4.5 and RCP8.5 scenarios in 2070 on forest increment under the influence of various biotic and abiotic factors. Different structures of the ANN model were developed due to its ability to model nonlinear relationships. The most important factor in tree increment was elevation and BAL. The effect of climate, which included an increase in precipitation and temperature at the end of the study period, on increment was not very noticeable. In fact, many factors affect the response of tree increment to climate change, such as species type, site conditions, and tree age. Our results demonstrated that the effect of increasing temperature, which reduces the increment rate, is accompanied by an increase in precipitation, which increases the increment rate. These climatic factors neutralize the effect on the increment rate and, therefore, the increment rate does not change significantly at the end of the period compared to the beginning.

Supplementary Materials: The following supporting information can be downloaded at: https://www.mdpi.com/article/10.3390/f13111816/s1, Table S1: The results of the MLP model for the training step; Table S2. The results of the MLP model for the validation step; Table S3. Characteristics of RBF and MLP-based ANNs and associated metrics for diameter model training; Table S4 Characteristics of RBF and MLP-based ANNs and associated metrics for diameter model evaluation.

Author Contributions: M.B. conceived and designed the experiments; M.B., S.K.H., and S.H. performed the experiments and analyzed the data; M.B. and S.K.H. contributed reagents/materials/analysis tools; M.B., T.K., H.B., and A.J. wrote the paper. All authors have read and agreed to the published version of the manuscript.

Funding: This research received no external funding.

Institutional Review Board Statement: Not applicable.

Informed Consent Statement: Not applicable.

Data Availability Statement: The data underlying this article will be shared on reasonable request to the corresponding author.

Conflicts of Interest: None of the authors have any actual or potential conflict of interest that could inappropriately influence, or be perceived to influence, this work.

References

1. Yue, Z.; Zhou, W.; Li, T. Impact of the Indian Ocean dipole on evolution of the subsequent ENSO: Relative roles of dynamic and thermodynamic processes. *J. Clim.* **2021**, *34*, 3591–3607. [CrossRef]
2. Longo, M.; Knox, R.G.; Levine, N.M.; Alves, L.F.; Bonal, D.; Camargo, P.B.; Fitzjarrald, D.R.; Hayek, M.N.; Restrepo-Coupe, N.; Saleska, S.R. Ecosystem heterogeneity and diversity mitigate Amazon forest resilience to frequent extreme droughts. *New Phytol.* **2018**, *219*, 914–931. [CrossRef] [PubMed]
3. Hamidi, S.K.; de Luis, M.; Bourque, C.P.-A.; Bayat, M.; Serrano-Notivoli, R. Projected biodiversity in the Hyrcanian Mountain Forest of Iran: An investigation based on two climate scenarios. *Biodivers. Conserv.* **2022**, 1–18. [CrossRef]
4. Quan, Q.; Liang, W.; Yan, D.; Lei, J. Influences of joint action of natural and social factors on atmospheric process of hydrological cycle in Inner Mongolia, China. *Urban Clim.* **2022**, *41*, 101043. [CrossRef]
5. Tollefson, J. IPCC climate report: Earth is warmer than it's been in 125,000 years. *Nature* **2021**, *596*, 171–172. [CrossRef]
6. Lo Piccolo, E.; Landi, M. Red-leafed species for urban "greening" in the age of global climate change. *J. For. Res.* **2021**, *32*, 151–159. [CrossRef]
7. Crookston, N.L.; Rehfeldt, G.E.; Dixon, G.E.; Weiskittel, A.R. Addressing climate change in the forest vegetation simulator to assess impacts on landscape forest dynamics. *For. Ecol. Manag.* **2010**, *260*, 1198–1211. [CrossRef]
8. Littell, J.S.; McKenzie, D.; Kerns, B.K.; Cushman, S.; Shaw, C.G. Managing uncertainty in climate-driven ecological models to inform adaptation to climate change. *Ecosphere* **2011**, *2*, 1–19. [CrossRef]
9. Escoriza, D.; Hernandez, A. Buffered microclimate determines the presence of Salamandra corsica. *J. For. Res.* **2021**, *32*, 1089–1093. [CrossRef]
10. Kirschbaum, M.U. Forest growth and species distribution in a changing climate. *Tree Physiol.* **2000**, *20*, 309–322. [CrossRef]
11. Yang, Y.; Li, T.; Wang, Y.; Cheng, H.; Chang, S.X.; Liang, C.; An, S. Negative effects of multiple global change factors on soil microbial diversity. *Soil Biol. Biochem.* **2021**, *156*, 108229. [CrossRef]
12. Limaki, M.K.; Nimvari, M.E.-h.; Alavi, S.J.; Mataji, A.; Kazemnezhad, F. Potential elevation shift of oriental beech (Fagus orientalis L.) in Hyrcanian mixed forest ecoregion under future global warming. *Ecol. Model.* **2021**, *455*, 109637. [CrossRef]
13. Yang, Y.; Li, T.; Pokharel, P.; Liu, L.; Qiao, J.; Wang, Y.; An, S.; Chang, S.X. Global effects on soil respiration and its temperature sensitivity depend on nitrogen addition rate. *Soil Biol. Biochem.* **2022**, *174*, 108814. [CrossRef]
14. Strömgren, M.; Linder, S. Effects of nutrition and soil warming on stemwood production in a boreal Norway spruce stand. *Glob. Change Biol.* **2002**, *8*, 1194–1204. [CrossRef]
15. Yang, Y.; Watanabe, M.; Li, F.; Zhang, J.; Zhang, W.; Zhai, J. Factors affecting forest growth and possible effects of climate change in the Taihang Mountains, northern China. *For. Int. J. For. Res.* **2006**, *79*, 135–147. [CrossRef]
16. Dunn, R.J.; Hurst, D.F.; Gobron, N.; Willett, K.M. Global climate [in "state of the climate in 2016"]. *Bull. Amer. Meteor. Soc* **2017**, *98*, 5–62.
17. Jactel, H.; Koricheva, J.; Castagneyrol, B. Responses of forest insect pests to climate change: Not so simple. *Curr. Opin. Insect Sci.* **2019**, *35*, 103–108. [CrossRef]
18. Coelho, L.; Nascimento, A.R.T.; Santos, J.C.; Silva, V.F. Unveiling an important interaction in forestry: Ectomyelois muriscis and Khaya grandifoliola cankers and tree growth. *J. For. Res.* **2021**, *32*, 1287–1293. [CrossRef]
19. Li, W.; Shi, Y.; Zhu, D.; Wang, W.; Liu, H.; Li, J.; Shi, N.; Ma, L.; Fu, S. Fine root biomass and morphology in a temperate forest are influenced more by the nitrogen treatment approach than the rate. *Ecol. Indic.* **2021**, *130*, 108031. [CrossRef]
20. Ashraf, M.I.; Meng, F.-R.; Bourque, C.P.-A.; MacLean, D.A. A novel modelling approach for predicting forest growth and yield under climate change. *PLoS ONE* **2015**, *10*, e0132066. [CrossRef]
21. Hamidi, S.K.; Weiskittel, A.; Bayat, M.; Fallah, A. Development of individual tree growth and yield model across multiple contrasting species using nonparametric and parametric methods in the Hyrcanian forests of northern Iran. *Eur. J. For. Res.* **2021**, *140*, 421–434. [CrossRef]
22. Pretzsch, H.; Bielak, K.; Block, J.; Bruchwald, A.; Dieler, J.; Ehrhart, H.-P.; Kohnle, U.; Nagel, J.; Spellmann, H.; Zasada, M. Productivity of mixed versus pure stands of oak (Quercus petraea (Matt.) Liebl. and Quercus robur L.) and European beech (Fagus sylvatica L.) along an ecological gradient. *Eur. J. For. Res.* **2013**, *132*, 263–280. [CrossRef]
23. Adeniyi, M.O. The consequences of the IPCC AR5 RCPs 4.5 and 8.5 climate change scenarios on precipitation in West Africa. *Clim. Change* **2016**, *139*, 245–263. [CrossRef]
24. Yang, Y.; Chen, X.; Liu, L.; Li, T.; Dou, Y.; Qiao, J.; Wang, Y.; An, S.; Chang, S.X. Nitrogen fertilization weakens the linkage between soil carbon and microbial diversity: A global meta-analysis. *Glob. Change Biol.* **2022**, *28*, 6446–6461. [CrossRef] [PubMed]
25. Bayat, M.; Pukkala, T.; Namiranian, M.; Zobeiri, M. Productivity and optimal management of the uneven-aged hardwood forests of Hyrcania. *Eur. J. For. Res.* **2013**, *132*, 851–864. [CrossRef]
26. Hamidi, S.K.; Zenner, E.K.; Bayat, M.; Fallah, A. Analysis of plot-level volume increment models developed from machine learning methods applied to an uneven-aged mixed forest. *Ann. For. Sci.* **2021**, *78*, 4. [CrossRef]
27. Bayat, M.; Burkhart, H.; Namiranian, M.; Hamidi, S.K.; Heidari, S.; Hassani, M. Assessing biotic and abiotic effects on biodiversity index using machine learning. *Forests* **2021**, *12*, 461. [CrossRef]
28. Bourque, C.P.-A.; Bayat, M. Landscape variation in tree species richness in northern Iran forests. *PLoS ONE* **2015**, *10*, e0121172. [CrossRef]

29. Munyasya, A.N.; Koskei, K.; Zhou, R.; Liu, S.-T.; Indoshi, S.N.; Wang, W.; Zhang, X.-C.; Cheruiyot, W.K.; Mburu, D.M.; Nyende, A.B. Integrated on-site & off-site rainwater-harvesting system boosts rainfed maize production for better adaptation to climate change. *Agric. Water Manag.* **2022**, *269*, 107672.
30. Tian, H.; Qin, Y.; Niu, Z.; Wang, L.; Ge, S. Summer Maize Mapping by Compositing Time Series Sentinel-1A Imagery Based on Crop Growth Cycles. *J. Indian Soc. Remote Sens.* **2021**, *49*, 2863–2874. [CrossRef]
31. Bayat, M.; Bettinger, P.; Hassani, M.; Heidari, S. Ten-year estimation of Oriental beech (Fagus orientalis Lipsky) volume increment in natural forests: A comparison of an artificial neural networks model, multiple linear regression and actual increment. *For. Int. J. For. Res.* **2021**, *94*, 598–609. [CrossRef]
32. Burkhart, H.E.; Tomé, M. *Modeling Forest Trees and Stands*; Springer Science & Business Media: Cham, Switzerland, 2012.
33. Chen, J.; Du, L.; Guo, Y. Label constrained convolutional factor analysis for classification with limited training samples. *Inf. Sci.* **2021**, *544*, 372–394. [CrossRef]
34. Liu, Y.; Zhang, K.; Li, Z.; Liu, Z.; Wang, J.; Huang, P. A hybrid runoff generation modelling framework based on spatial combination of three runoff generation schemes for semi-humid and semi-arid watersheds. *J. Hydrol.* **2020**, *590*, 125440. [CrossRef]
35. Zhou, R.; Wu, D.; Zhou, R.; Fang, L.; Zheng, X.; Lou, X. Estimation of DBH at forest stand level based on multi-parameters and generalized regression neural network. *Forests* **2019**, *10*, 778. [CrossRef]
36. García-Gutiérrez, J.; Martínez-Álvarez, F.; Troncoso, A.; Riquelme, J.C. A comparison of machine learning regression techniques for LiDAR-derived estimation of forest variables. *Neurocomputing* **2015**, *167*, 24–31. [CrossRef]
37. Kuehne, C.; Russell, M.; Weiskittel, A.; Kershaw, J., Jr. Comparing strategies for representing individual-tree secondary growth in mixed-species stands in the Acadian Forest region. *For. Ecol. Manag.* **2020**, *459*, 117823. [CrossRef]
38. Kweon, D.; Comeau, P.G. Relationships between tree survival, stand structure and age in trembling aspen dominated stands. *For. Ecol. Manag.* **2019**, *438*, 114–122. [CrossRef]
39. Primicia, I.; Camarero, J.J.; Janda, P.; Čada, V.; Morrissey, R.C.; Trotsiuk, V.; Bače, R.; Teodosiu, M.; Svoboda, M. Age, competition, disturbance and elevation effects on tree and stand growth response of primary Picea abies forest to climate. *For. Ecol. Manag.* **2015**, *354*, 77–86. [CrossRef]
40. Askarizadeh, D.; Arzani, H.; Jafary, M.; Bazrafshan, J.; Prentice, I.C. Surveying of the past, present, and future of vegetation changes in the central Alborz ranges in relation to climate change. *J. RS GIS Nat. Resour.* **2018**, *9*, 1–18.
41. Burkhart, H.E.; Brooks, E.B.; Dinon-Aldridge, H.; Sabatia, C.O.; Gyawali, N.; Wynne, R.H.; Thomas, V.A. Regional simulations of loblolly pine productivity with CO2 enrichment and changing climate scenarios. *For. Sci.* **2018**, *64*, 349–357. [CrossRef]
42. Subedi, N.; Sharma, M. Climate-diameter growth relationships of black spruce and jack pine trees in boreal Ontario, Canada. *Glob. Change Biol.* **2013**, *19*, 505–516. [CrossRef] [PubMed]
43. Sharma, M. Modelling climate effects on diameter growth of red pine trees in boreal Ontario, Canada. *Trees For. People* **2021**, *4*, 100064. [CrossRef]
44. Wilmking, M.; Juday, G.P. Longitudinal variation of radial growth at Alaska's northern treeline—Recent changes and possible scenarios for the 21st century. *Glob. Planet. Change* **2005**, *47*, 282–300. [CrossRef]
45. Goldblum, D.; Rigg, L. Tree growth response to climate change at the deciduous boreal forest ecotone, Ontario, Canada. *Can. J. For. Res.* **2005**, *35*, 2709–2718. [CrossRef]
46. Oboite, F.O.; Comeau, P.G. Climate sensitive growth models for predicting diameter growth of western Canadian boreal tree species. *For. Int. J. For. Res.* **2021**, *94*, 363–373. [CrossRef]
47. Laubhann, D.; Sterba, H.; Reinds, G.J.; De Vries, W. The impact of atmospheric deposition and climate on forest growth in European monitoring plots: An individual tree growth model. *For. Ecol. Manag.* **2009**, *258*, 1751–1761. [CrossRef]